Unit-Cell Analysis of Plasma-Excitation Slotted Waveguide Arrays Using Measured Electron Density and Temperature

Takuichi Hirano [1], Jiro Hirokawa [2], Makoto Ando [2]
[1]*Department of International Development Engineering, Tokyo Institute of Technology*
2-12-1-S3-19, O-okayama, Meguro-ku, Tokyo, 152-8552, JAPAN, E-mail: hira@antenna.ee.titech.ac.jp
[2]*Deptartment of Electrical and Electronic Engineering, Tokyo Institute of Technology*
E-mail: {jiro, mando}@antenna.ee.titech.ac.jp

Abstract

A unit-cell of plasma-excitation slotted waveguide arrays is analyzed by the GSM-MoM/FDTD hybridization method. In the GSM method, S-parameters of the analysis model are calculated by connecting S-parameters of subdivided blocks. S-parameters of vacuum window including plasma are analyzed by the FDTD method together with discretized motion equation for the electron. Measured electron density and temperature are used as macroscopic plasma parameter in the FDTD analysis of plasma as well as spatial gradation of plasma parameters.

1. INTRODUCTION

The authors have proposed a plasma equipment using slotted waveguide arrays [1][2] as shown in Fig.1. Microwave at 2.45GHz is used for the excitation. The unit-cell of the array, which is used for the array design, is analyzed by the generalized scattering matrix method (GSM) [3]-the method of moments (MoM) hybridization method by neglecting plasma [2]. Uniform aperture electromagnetic (EM) field distribution on the vacuum window (Plane A in Fig.1) is obtained [2]. Even if the uniform EM distribution is obtained, the realization of uniform plasma density distribution is difficult. And the analysis and design including plasma is necessary.

In this paper, plasma in the unit-cell of the array, as shown in Fig.2, is analyzed by the FDTD [4] with discretized Langevin equation, which is the motion equation for electron [5]. Then, the total characteristic of the unit-cell is analyzed by the GSM-MoM/FDTD hybridization method. S-matrix of the waveguide discontinuity in the vacuum window (Block7 in Fig.2(d)) is analyzed by the FDTD method in the presence of plasma. Measured electron density and temperature [1] (Fig.3), which are macroscopic parameters of plasma, are used as parameters in the analysis. As shown in Fig.3, the measured electron density and temperature decreases as the distance from the window (Plane A in Fig.1) increases. The real spatial gradation of plasma parameters can be considered by using the measured values.

S-matrix of the vacuum window including plasma (Block7 in Fig.2(d)) is analyzed by the FDTD. And the total characteristic of the unit-cell is calculated by connecting the S-matrices of all the Blocks.

2. ANALYSIS

A. FDTD Analysis for Plasma

Fig.3 shows the measured plasma characteristics by Langmiur probe [1]. The surface wave plasma (SWP), in which high electron density beyond cutoff is realized, is obtained. In this plasma, drift velocity of the heavy ion is negligible, which is referred to as cold plasma, because it is excited by very high frequency and the exchange of the kinetic momentum between the light electron and heavy ion is very small [6]. In cold plasma, only the motion equation for the electron, which is referred to as Langevin equation, is considered.

$$m_e \frac{d\mathbf{v}}{dt} = -e\mathbf{E} - m_e \nu_e \mathbf{v} \tag{1}$$

where e is the elementary charge. m_e, $\mathbf{v}$ and ν_e are mass, drift velocity and collision frequency of the electron, respectively. $\mathbf{E}$ is the electric field. The collision frequency of the electron ν_e can be written using gas (Ar) density n_0, collision cross section σ_e and thermal velocity of electron $\bar{v}_e$ [6].

$$\nu_e = n_0 \sigma_e \bar{v}_e \tag{2}$$

Only the collision between the electron and Ar is considered because this plasma is weakly ionized. Though σ_e is a function of electron energy, it is reported that $\sigma_e \cong 1.0\times10^{-19}[m^2]$ gives reasonable result [5], and this approximation is used in the report. The thermal velocity of electron $\bar{v}_e$ can be written using electron temperature T_e [6].

$$\bar{v}_e = \sqrt{\frac{8\kappa T_e}{\pi m_e}} \tag{3}$$

where κ is Boltzmann constant. Plasma current is calculated as follows.

$$\mathbf{i}_p = -en_e\mathbf{v} \tag{4}$$

where n_e is electron density. By solving Eq.(4) for $\mathbf{v}$ and substituting into Eq.(1), the differential equation for plasma current is obtained as follows.

$$\frac{d\mathbf{i}_p}{dt} = -\nu_e \mathbf{i}_p + \varepsilon_0 \omega_{pe}{}^2 \mathbf{E} \qquad (5)$$

where $\omega_{pe} = \sqrt{(n_e e^2)/(m_e \varepsilon_0)}$ (ε_0: permittivity of vacuum) is electron plasma angular frequency. $\mathbf{i}_p$ is discretized in time-domain $\mathbf{i}_p\big|_{t=n\Delta t} \equiv \mathbf{i}_p^n \cong \frac{\mathbf{i}_p^{n+1/2} + \mathbf{i}_p^{n-1/2}}{2}$ with the same method as the FDTD, and the central difference $\left.\frac{d\mathbf{i}_p}{dt}\right|_{t=n\Delta t} \cong \frac{\mathbf{i}_p^{n+1/2} - \mathbf{i}_p^{n-1/2}}{\Delta t}$ is used for time derivative. Then, the update equation for $\mathbf{i}_p^{n+1/2}$ is obtained as follows.

$$\mathbf{i}_p{}^{n+1/2} = \frac{1-\nu\Delta t/2}{1+\nu\Delta t/2}\mathbf{i}_p{}^{n-1/2} + \frac{\varepsilon_0 \omega_{pe}{}^2 \Delta t}{1+\nu\Delta t/2}\mathbf{E}^n \qquad (6)$$

$\mathbf{i}_p{}^{n+1/2}$ is updated in the same time as the magnetic field $\mathbf{H}^{n+1/2}$, and is spatially arranged in the same position as the electric field $\mathbf{E}^n$ in Yee-cell.

B. GSM-MoM/FDTD Analysis for a Unit-Cell

A unit-cell of plasma excitation slotted waveguide arrays is shown in Fig.2. In the GSM analysis [3], the original structure is decomposed into several blocks. Then, S-matrix of each block is calculated and the scattering characteristic of the original structure is calculated by connecting the S-matrices. S-matrices of Blocks from 1 to 6 in Fig.2 (d) are analyzed by the MoM, and that of Block 7 is analyzed by the proposed FDTD analysis in the presence of plasma. S-matrix of Block7, which is a multimode waveguide, is analyzed by the method in reference [7]. The measured electron density and temperature, as shown in Fig.3, are used in the FDTD analysis, and n_e in Eq.(4) and T_e in Eq.(3) can be determined.

3. NUMERICAL RESULTS

A. FDTD Analysis for Block7 in Fig.2

Fig.4 shows the FDTD analysis model of Block7 in Fig.2 (*h*=0mm, without Plasma) and the calculated electric-field magnitude. Absorbing boundary conditions (ABCs) are implemented in the terminals of Port1 and Port2 in order to simulate the infinitely-long waveguide. Fig.5 shows analytically-derived all the propagating modes of Port1 in Fig.4. The excitation in Fig.4 is the dominant TEM mode (Mode1). Vertical walls of the waveguide are perfect electric conductors (PECs) and the horizontal ones are periodic boundary conditions (PBCs).

Fig.6 shows frequency characteristic of reflection coefficient $S_{11,11}$ for Block7, where $S_{ap,bq}$ indicates the S-parameter with the ratio of reflected Mode *p* in Port *a* against the incidence of Mode *q* in Port *b*. The agreement between the results by the FDTD and MoM [2] is reasonable.

B. GSM-MoM/FDTD Analysis for a Unit-Cell without Plasma

Fig.7 shows the frequency characteristic of transmission coefficient S_{21} for the unit-cell in Fig.2 (*h*=0mm, without Plasma, *p*=20mm, *l*=64mm, *w*=5mm). The phase reference plane is indicated in Fig.2(c). In S-matrix of Block7, only Mode1, 5 and 13 are considered because they are the entire scattered fields which are created by the dominant TEM mode (Mode1) with considering symmetrical structure at the discontinuity. The result of the GSM-MoM/FDTD agrees very well with that of the GSM-MoM. When the S-matrix of Block7 is set to be zero, the result is changed, and it is concluded that the effect of the Block7 is not negligible and the validity of the GSM-MoM/FDTD is confirmed.

C. Plasma Analysis using FDTD

Fig.8 shows a numerical example of plasma analysis using FDTD, which is explained in Sec.2. The waveguide walls are consisting of PEC walls and periodic boundary walls, which simulates a parallel plate waveguide. The CW source is excited by a TEM-shaped current sheet at 2.45GHz. The electric field distribution with variation of plasma density is described in the figure. The equivalent relative complex permittivity of plasma ε_{rp} is expressed as follows.

$$\varepsilon_{rp} = 1 - \frac{\omega_{pe}{}^2}{\omega(\omega - j\nu_e)} \qquad (7)$$

When $\nu_e = 0$, ε_{rp} becomes smaller than 1. When $\varepsilon_{rp} = 0$, or $\omega = \omega_{pe}$, it is called cutoff. The extension of the wavelength and cutoff around the cutoff density of $n_e = 7.45\times10^{16}$ [m^{-3}] are properly observed in the figure.

D. GSM-MoM/FDTD Analysis for Unit-Cell with Plasma

Fig.9 shows the reflection coefficient $S_{11,11}$ of Block7 as a function of glass thickness *h*. Plasma layer is modelled outside the vacuum window within the length of 400mm from the glass, which is referred to as *(plasma: graded,* l_p *=400mm)* hereafter. Plasma parameters n_e and T_e are given by an approximated least square curve for the measured values (Fig.3), and spatial gradation of plasma parameter is taken into account in the analysis. The reflection becomes larger in the presence of plasma than that of -10dB without plasma (Fig.6). When *h*=10mm, the reflection becomes minimum of about -1.5dB, and this parameter is used hereafter.

Fig.10 shows the reflection coefficient $S_{11,11}$ of Block7 as a function of the collision cross section σ_e. In plasma, there are electrons with various energy, and their σ_e are different because σ_e is a function of electron energy [6]. The average

value of σ_e is used in the analysis. Fig.10 guarantees that the assumption of $\sigma_e \cong 1.0\times10^{-19}[m^2]$ is reasonable [5] because the change of $S_{11,11}$ is very small with variation of σ_e.

Fig.11 shows the reflection coefficient $S_{11,11}$ of Block7 as a function of the thickness of plasma layer l_p (plasma: graded, l_p). When l_p becomes larger than 10mm, $S_{11,11}$ converges to that of plasma model (graded, l_p =400mm). And $S_{11,11}$ of the model (graded, l_p =400mm) is considered to be well converged.

Fig.12 shows the reflection coefficient $S_{11,11}$ of Block7 as a function of the electron density n_e filled with uniform density plasma. $n_e = 8.44\times10^{12}[cm^{-3}]$ is the maximum density, which is used in the model (graded, l_p =400mm). The graph means that the graded plasma model (graded, l_p =400mm) can be replaced with the uniform plasma model with the plasma parameter at the vacuum window. The graph also shows the tolerance of the plasma parameter.

Fig.13 shows a snapshot of electric field and plasma current in Block7 (h=10mm, plasma: graded, l_p =400mm). It is observed that the electric field can not penetrate into plasma, and there is plasma current near the surface of the vacuum window.

Tab.1 shows S-parameter of the unit-cell in Fig.2. When plasma exists, the reflection S_{11} and transmission S_{21} increases, and the coupling power to the port 3 decreases.

4. CONCLUSION

A unit-cell of plasma-excitation slotted waveguide arrays is analyzed by the GSM-MoM/FDTD hybridization analysis. S-matrix of vacuum window including plasma is analyzed by the FDTD together with discretized motion equation for the electron. The accuracy of the GSM-MoM/FDTD hybridization analysis is confirmed by comparing with the GSM-MoM. The result shows that the reflection and transmission coefficients of a unit-cell become large in the presence of plasma. The design of the array in the presence of plasma will be the future study.

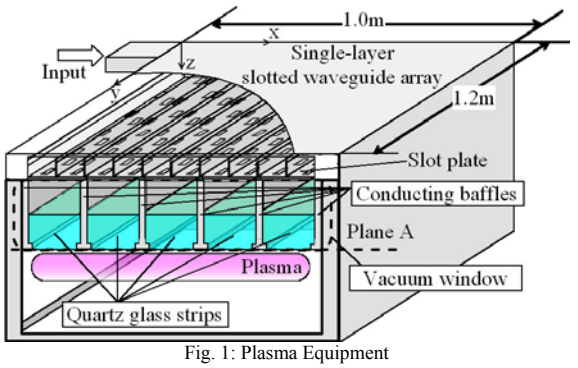

Fig. 1: Plasma Equipment

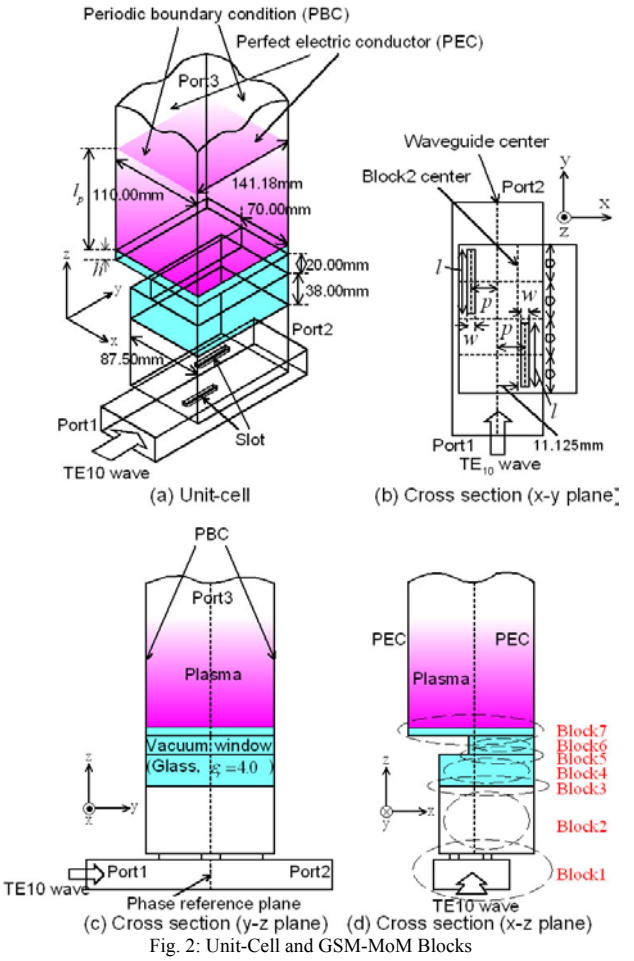

Fig. 2: Unit-Cell and GSM-MoM Blocks

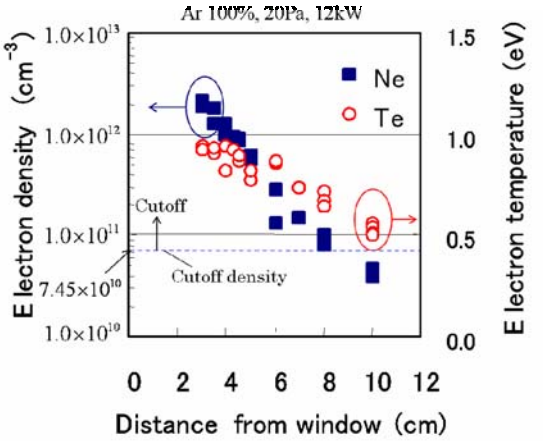

Fig. 3: Measured Electron Density and Electron Temperature as a Function of the Distance from Window (Plane A in Fig.1) [1]

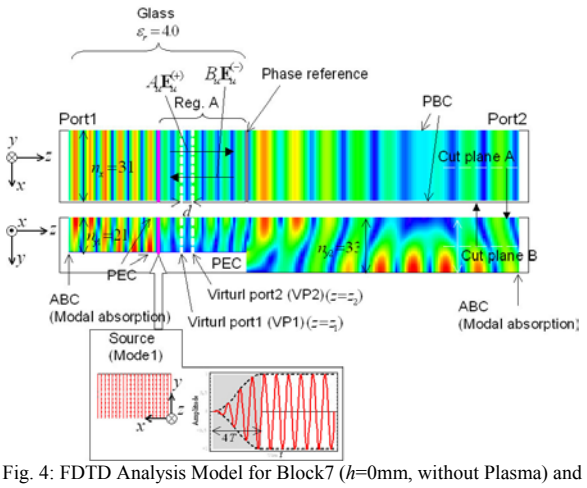

Fig. 4: FDTD Analysis Model for Block7 (h=0mm, without Plasma) and Calculated Electric-Field Magnitude

TE(H) mode

m \ n	0	1	2
0	Mode1	Mode4	Mode12
1	Mode2 (Re) Mode3 (Im)	Mode6 (Re) Mode7 (Im)	Mode18 (Re) Mode19 (Im)
2	Mode10 (Re) Mode11 (Im)	Mode14 (Re) Mode15 (Im)	

TM(E) mode

m \ n	0	1	2
0		Mode5	Mode13
1		Mode8 (Re) Mode9 (Im)	Mode20 (Re) Mode21 (Im)
2		Mode16 (Re) Mode17 (Im)	

Fig. 5: Analytically-Derived Propagating Modes of Port1 in Block7

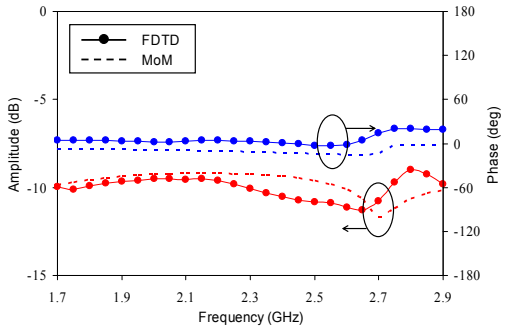

Fig. 6: Frequency Characteristic of $S_{11,11}$ for Block7 (h=0mm, without Plasma)

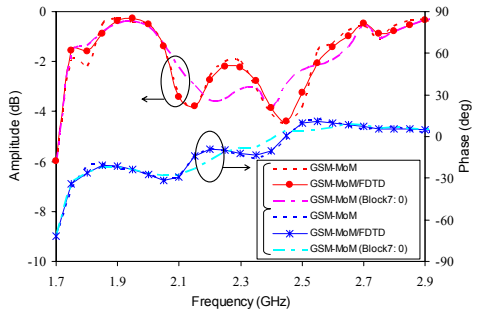

Fig. 7: Frequency Characteristic of Transmission Coefficient S_{21} for the Unit-Cell
(h=0mm, without Plasma, p=20mm, l=64mm, w=5mm)

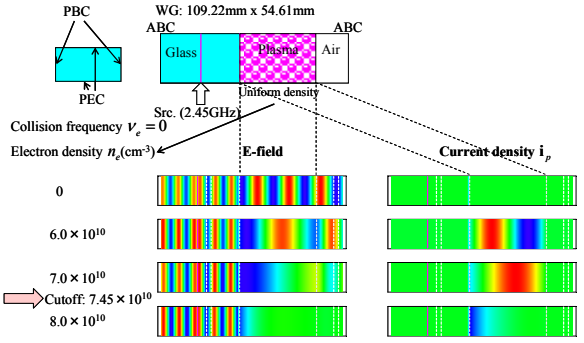

Fig. 8: Plasma Analysis using FDTD ($\nu_e = 0$)

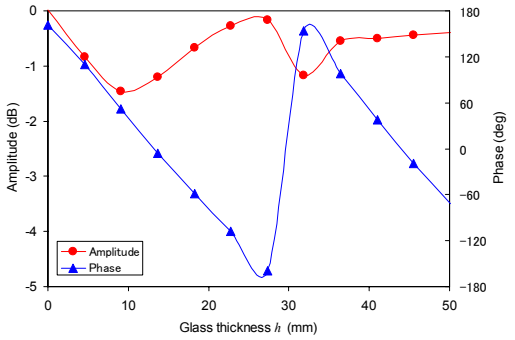

Fig. 9: Reflection Coefficient $S_{11,11}$ of Block7 as a Function of Glass Thickness h (plasma: graded, l_p=400mm)

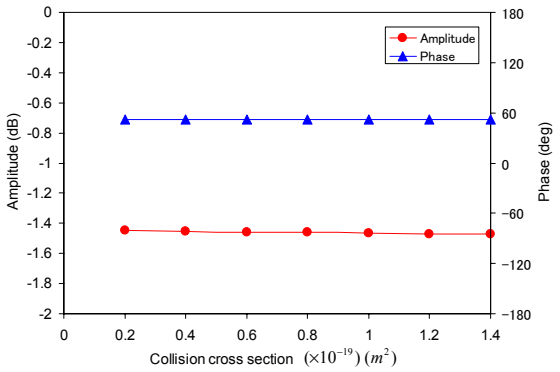

Fig. 10: Reflection Coefficient $S_{11,11}$ of Block7 as a Function of Collision Cross Section (h=10mm, plasma: graded, l_p=400mm)

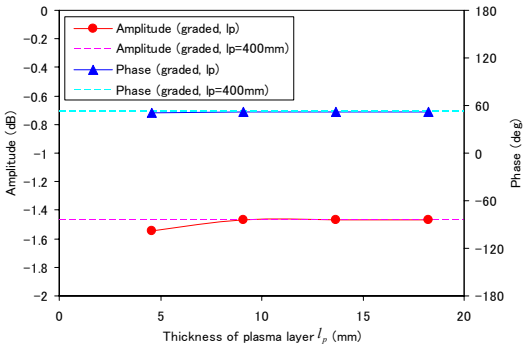

Fig. 11: Reflection Coefficient $S_{11,11}$ of Block7 as a Function of Thickness of Plasma Layer l_p (h=10mm)

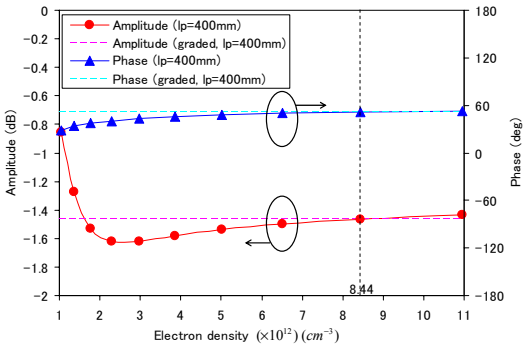

Fig. 12: Reflection Coefficient $S_{11,11}$ of Block7 as a Function of Electron Density filled with Uniform Density Plasma (h=10mm)

TABLE 1: S-PARAMETER OF UNIT-CELL

	S_{11}		S_{21}	
	dB	deg	dB	deg
h=0, w/o plasma	-9.63	-6.16	-4.47	-2.16
h=10mm, w/ plasma (graded, l_p=400mm)	-5.94	47.64	-1.91	-30.24

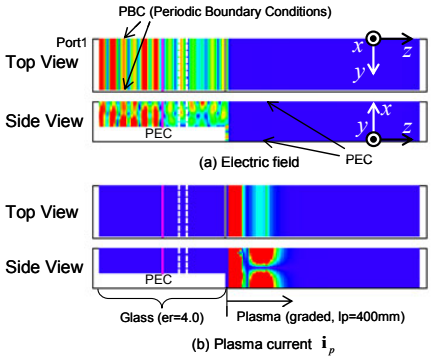

Fig. 13: Snapshot of Electric Field and Plasma Current in Block7 (h=10mm, plasma: graded, l_p=400mm) Calculated by the FDTD

REFERENCES

[1] M. Goto, A. Sasaki, T. Okamoto, K. Azuma, Y. Nakata, T. Hirano, and M. Ando, "New plasma processing equipment for large-size displays using single-layer slotted waveguide array and application to plasma oxidation for LTPS-TFTs," International Workshop on Active-Matrix Liquid-Crystal Displays (AM-LCD'03), pp.99-102, July 2003.

[2] T. Hirano, K. Sakurai, J. Hirokawa, M. Ando, T. Ide, A. Sasaki, K. Azuma, and Y. Nakata, "Design of 1m^2 order plasma excitation single-layer slotted waveguide array with conducting baffles and quartz glass strips using the GSM-MoM analysis," IEICE Trans. Commun., vol.E89-B, no.5, pp.1627-1635, May 2006.

[3] A.I. Khalil, and M.B. Steer, "A generalized scattering matrix method using the method of moments for electromagnetic analysis of multilayered structures in waveguide," IEEE Trans. Microwave Theory and Techniques, vol.47, no.11, pp.2151-2157, Nov. 1999.

[4] K.S. Kunz and R.J. Luebbers, Finite Difference Time Domain Method for Electromagnetics, CRC Press, Inc., Boca Raton, 2003.

[5] C. Qing, P.H. Aoyagi, and M. Katsurai, "Numerical analysis of surface wave excitation in a planar-type nonmagnetized plasma processing device," IEEE Trans. Plasma Science, vol.27, no.1, pp.164-170, Feb. 1999.

[6] H. Sugai, Plasma Electronics, Ohmsha, Tokyo, 2003. (in Japanese)

[7] T. Hirano, A. Nishikata, J. Hirokawa, and M. Ando, "FDTD analysis of S-Parameters for a multi-mode waveguide with CW excitation," IEEE AP-S Digest, Session: 267.7, pp.1587-1590, Albuquerque, NM, USA, July 9-14, 2006.